

On the linkage of impact damage to modeling of ballistic performance

J. M. Wells

JMW Associates, Mashpee, MA, USA

Abstract

The assessment of terminal ballistic performance has historically been strongly biased toward the penetration resistance of the target architecture and its component materials. However, penetration modeling alone does not provide sufficient knowledge to create new and/or improved armor ceramics materials capable of mitigating and preventing penetration. It is apparent that physical impact damage occurs prior to, and strongly affects, the occurrence and progress of the penetration process and as such impact damage needs to be explicitly included in ballistic performance modeling. One aspect of this situation has been the difficulty in attaining a detailed volumetric characterization of actual sub-surface bulk impact damage. The x-ray computed tomography, XCT, diagnostic and 3D visualization techniques presently appear as the only effective nondestructive evaluation, NDE, modality for high resolution volumetric impact damage interrogation, spatial characterization, quantification, visualization, and 3D analysis. An overview of the current XCT impact damage diagnostic capabilities and results are discussed along with some remaining challenges and the need to incorporate 3D physical damage features into future computational models for predictive ballistic performance.

Keywords: X-ray Computed Tomography, XCT, damage diagnostics, ballistic impact damage, computational modelling, terminal ballistics, NDE, cracking, embedded fragments, impact-induced porosity.

1 Introduction

The historical focus of ballistic computational modeling on the penetration phenomenon is understandable and logical in that no friendly armor system should be penetrated. However, penetration-only based models lack the



capability to provide the essential insight into extrinsic target architectural or intrinsic material modifications required for the design of vastly improved ceramic armor systems. Penetration models generally use a 2D axisymmetric geometry approach which has proven computationally tractable and successful in creating accurate penetration simulations. The measurement of penetration parameters is relatively straight forward and hence the validation and verification of penetration-only models is quite possible. Conversely, comparatively little progress has been made in developing physical damage-based computational models that accurately describe real ballistic impact damage.

It is apparent that physical impact damage occurs prior to, and likely affects, the occurrence and progress of the penetration process and as such needs to be explicitly included in ballistic performance modeling [1]. Impact damage has received renewed attention over the past decade with the evolution and application of non-invasive industrial x-ray computed tomography, XCT, damage diagnostic and 3D voxel visualization techniques. XCT presently appears as the only effective NDE modality for high resolution volumetric ballistic impact damage interrogation, spatial characterization, quantification, visualization, and 3D analysis and has been successfully demonstrated on armor ceramics [1-8] and Ti-6Al-4V monolithic metallic armor materials [9]. Its inclusion in predictive ballistic impact damage modeling [1,6] has been proposed.

2 Background

The traditional “post-mortem” method of examining ballistic damage within the interior of impacted opaque ceramic targets has been destructive metallographic sectioning, polishing, and optical and electron microscopy. While permitting damage observations at multiple length scales, this method is irreversible and is essentially limited to observations on individual 2-D planar sections. Traditional non-destructive examination, NDE, modalities such as digital x-ray and ultrasound are currently more capable of damage “detection” than they are of the detailed characterization of defect size, morphology, volumetric location, and the discrimination between multiple damage variants which are superimposed in a complex assemblage.

Thus an essential need exists for a diagnostic in-situ approach which can provide the qualitative and quantitative characterization details of actual impact-induced damage. The most satisfactory “post-mortem” solution demonstrated to fulfil this need to date is industrial x-ray computed tomography, XCT. Yet, other than the work of the author and/or his collaborators [1-9], no other published application of this approach for ceramic impact damage diagnostics is known.

3 XCT impact damage results

3.1 Impact damage

There is no universally agreed upon definition of impact damage in terminal ballistics testing of armor ceramics. Most of the post-mortem studies using



destructive metallographic sectioning focus their description of impact damage on traditional types of radial, ring, conical, and laminar cracking. These observations are made on a limited number of 2D planar sections and do not provide a full spatial characterization of these cracking types. Computational ballistic models such as the Johnson-Holmquist [10] model invoke a less physically descriptive, yet more mathematically convenient damage definition by relating cumulative inelastic strain to a normalized “damage function” which ranges from a value of 0 for no damage up to the fully damaged condition with a value of 1.0. The use of this simplistic damage definition has worked reasonably well for the computational model of the penetration phenomenon. Such mathematically unsophisticated definitions of impact damage do not incorporate the distinct differences in the various details of actual ballistic impact damage. Granted the inclusion of such realistic details of the actual physical impact damage is a most difficult computational modeling challenge. However, the author considers it ultimately necessary to achieve a computational methodology which more closely incorporates critical aspects of real impact damage features.

3.2 The XCT approach to impact damage diagnostics

XCT is a powerful and functional 3D NDE diagnostic modality which allows the in-situ interrogation of the external and internal design surfaces and/or damage features within the bulk of the original object. The triangulation of volumetric x-ray absorption data is utilized to construct a completely digitized “density” map of a solid object thus accurately representing the dimensional and structural features of that object. Resolution levels achievable with XCT are a function of both the object’s size and density, and the x-ray source and detector system. The nominal resolution level for the meso-scale tomography of a modest size medium density laboratory ballistic target is < 0.250 mm. Higher microtomography resolution levels of < 20 microns are achievable only on relatively less dense and/or smaller objects. If higher resolution levels are still required, then destructive sectioning and electron microscopy techniques may augment the results of XCT. After digitization of the physical target by XCT scanning, subsequent interrogations of the impacted target are then conducted in the *virtual* diagnostic domain. The original XCT scan data file is reconstructed into a virtual 3D solid object using an advanced voxel analysis and visualization software package [11]. Several sophisticated image processing tools and routines are then used to obtain the XCT diagnostic results that contribute to the enhanced understanding of various physical impact damage details. The XCT diagnostic results are reproducible, accessible, and amenable to digital archival file storage.

3.2.1 Impact damage observations in TiB_2

An earlier ballistic experiment conducted in 1996 at the US Army Research Laboratory involved a target of a short cylindrical TiB_2 ceramic measuring 72 mm in diameter by 25 mm in thickness [2,4]. Examples of some of the XCT diagnostic results obtained on this sample are shown in figures 1 to 4. Various impact surface and near-surface impact damage feature observations are shown in figure 1. Perhaps the most dramatic damage features shown here are the three



distinct circular “steps” which surround the large impact cavity. These steps appear to be an agglomeration of intermixed debris from both the impacting projectile and the target ceramic. The height of these steps decreases from ~3.5 mm for the inner circular step to ~ 1.2 mm for the outermost step. Their grey levels directly reflect their density which was found to be intermediate between that for the projectile and for the TiB_2 ceramic. Figure 2 reveals a large tungsten alloy projectile fragment mass and the segmented cracking impact damage features observed in a virtually transparent 3D view.

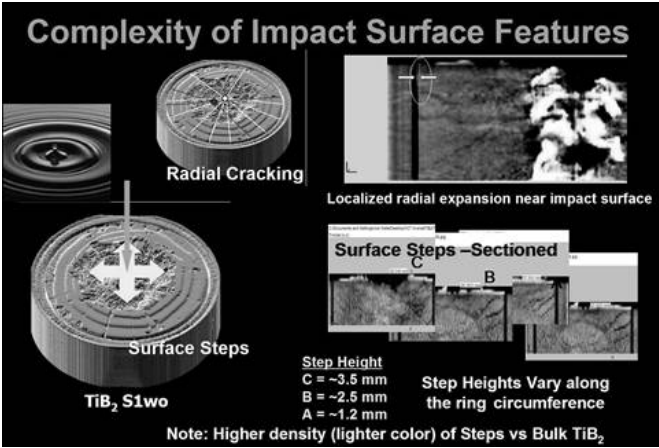


Figure 1: Examples of surface and near surface damage features.

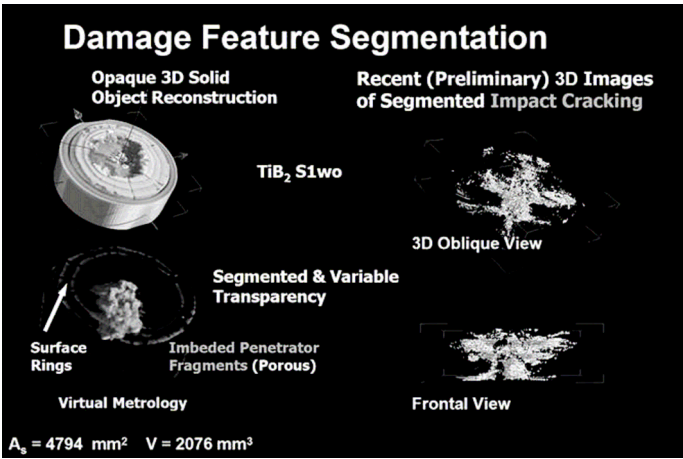


Figure 2: Segmented and virtual transparent views of a large projectile fragment mass and impact cracking.

Further investigation of the large embedded tungsten alloy projectile fragment revealed that it is not a homogeneous mass of projectile composition, but rather is a complex agglomeration of multiple small tungsten alloy fragments

intermixed with debris from both the ceramic rubble and fine rubble from the projectile. The intermixed debris is identified from its grey level (primarily a density indicator) found to be intermediate between that of the high density projectile material and the lower density of the host ceramic material. Also, the presence of impact-induced porosity was observed entrapped within the large agglomerated fragment mass. In figure 3 these features are observed in the virtual longitudinal section and the four axial slices taken at locations from above the exit face (A-20) to below the impact face (A-135).

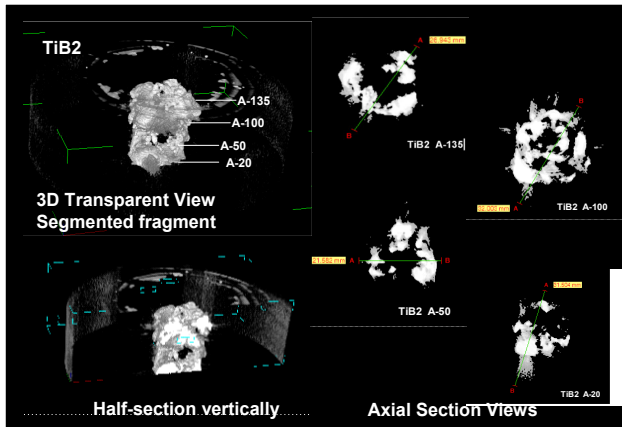


Figure 3: Fragment details revealing the multiple smaller w-alloy fragments (white) with enclosed porosity and intermixed ceramic debris (darker grey areas).

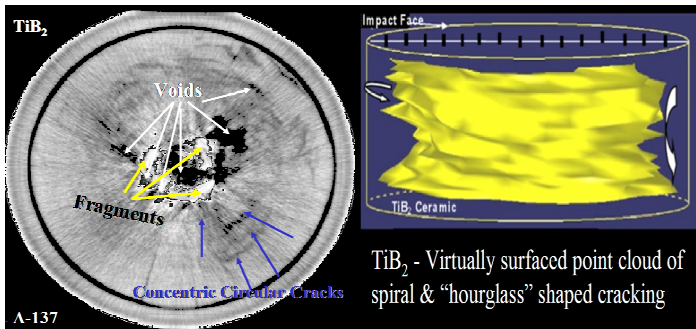


Figure 4: Three separate impact damage modes in the axial slice image on the left; both spiral and "hourglass" shaped cracking morphology is evident on the image on the right.

Two additional and very revealing images of damage features are shown in figure 4. First, the image on the left is an axial slice (A-137) of the TiB_2 target in which can be seen several small projectile fragments in the center of the sample.

Also seen in this image are several significant voids (dark grey level) about the embedded fragments. Finally, one can distinguish four concentric circular cracks surrounding the central voids and fragments. These circular cracks are actually the intersections of 3D conical cracks with the axial plane of this image. The image on the right side of figure 4 shows a profile view of a virtually surfaced point cloud of the complex cracking morphology within the TiB_2 ceramic. Two observations are made from this unique image: first that a spiral “thread-like” orientation of the cracking exists, and secondly that the cracking diameter is larger at both the impact and exit surfaces and narrows near the mid-thickness of the target. This narrowing “hourglass” shaped cracking profile likely results from the interaction of incident and reflective shock waves and demonstrates extremely complex cracking damage morphology.

3.2.2 Impact damage observations in Al_2O_3

Additional impacted ceramic targets examined include an Al_2O_3 target made available for XCT diagnostic study from the earlier work of D.A. Shockey et al. [12-14]. This target consisted of a half-cylindrical longitudinal section measuring approximately 100 mm in height by 102 mm in width. It has a large cavity on its impact surface and had been totally penetrated. Figure 5 includes virtual reconstructed images of this target revealing both the virtually segmented semi-continuous projectile fragments through the entire thickness of the target and the presence of an inhomogeneous distribution of impact-induced porosity in close proximity to the fragment segments. A further complexity of the fragment material is revealed in the virtual axial slices shown on the left hand side of figure 6. As observed in the smaller TiB_2 target above, the inner structure of the large fragment sections consists of multiple smaller tungsten alloy fragments (whitest grey levels) and intermixed debris of ceramic and projectile fine rubble.

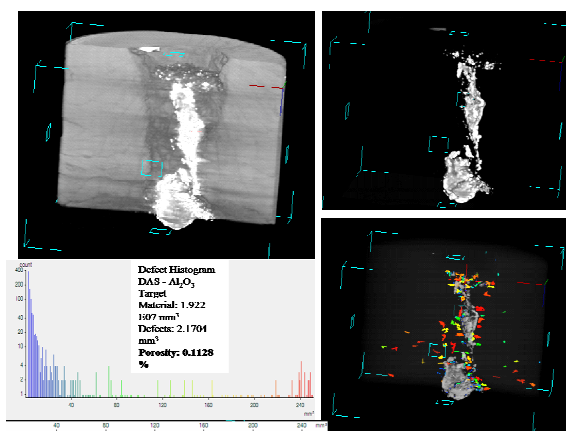


Figure 5: XCT virtual images showing segmented projectile fragments and adjacent impact-induced porosity.

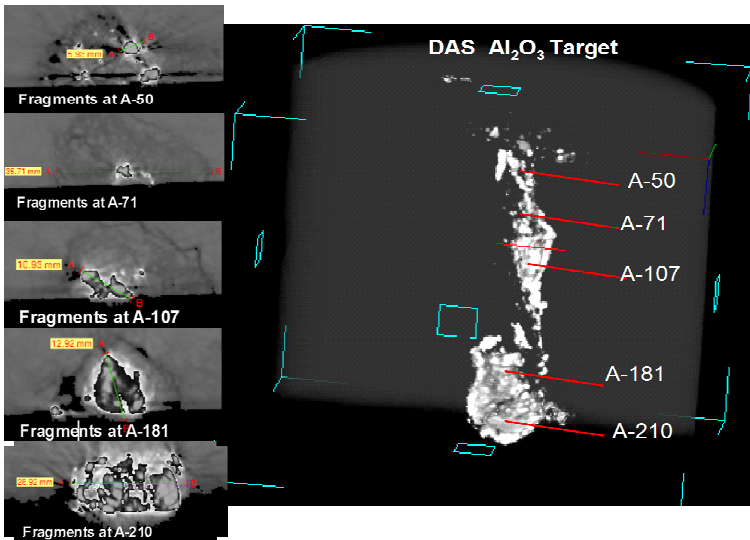


Figure 6: The complex inner-structure of the large fragment is revealed in the five designated virtual axial slices as shown on the left.

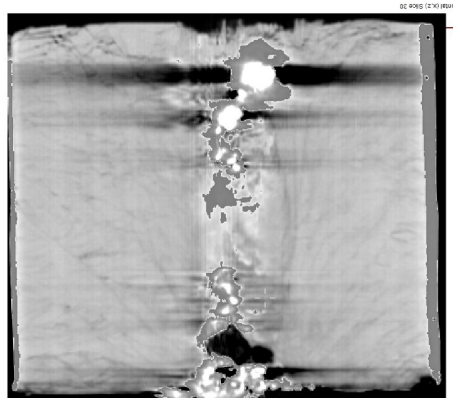


Figure 7: Frontal view of the B_4C ceramic target reveals several manifestations of impact damage.

3.2.3 Impact damage observations in B_4C

Another impacted ceramic target sample made available from the work of Shockey et al. [12-14] was a longitudinally sectioned half-cylindrical target of B_4C ceramic measuring approximately 113 mm in height by 103 mm in width. This target has a modest sized cavity on its impact surface and had also been fully penetrated by the high energy kinetic energy projectile. Several damage features are observed on the virtual rendered frontal section shown in figure 7 including multiple high density (bright white) projectile fragments, medium grey

intermixed areas of B_4C ceramic and finer tungsten alloy debris, and enclosed porosity (fully dark grey level). Impact-induced cracking, although in somewhat low contrast, is also observed. The large dark horizontal bands appearing in figure 7 occur at the identical heights as the larger high density fragments and are considered artifacts created in the original scanning process.

With the application of the virtual transparency image processing technique, the opacity of the B_4C ceramic is adjusted to zero and embedded fragment sections are observed discontinuously through the thickness of the target. Also, with the defect analysis tool, the presence of localized impact-induced porosity is seen adjacent to all major projectile fragments as shown in figure 8.

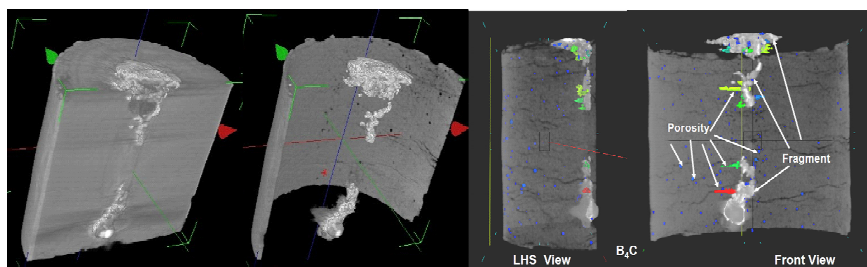


Figure 8: Oblique 3D images show segmented projectile fragments from the impact to the exit face. Images on the right show localized porosity adjacent to fragments.

3.3 Discussion of observed impact damage features

With the information developed from the above three impacted ceramic targets samples, as well as from additional targets examined by the author but not described herein, several somewhat revealing impact damage observations can be made as follows:

- Several types of physical ballistic impact damage occur in terminal ballistic ceramic targets, including complex cracking morphologies, impact-induced voids and porosity, and multiple embedded tungsten alloy projectile fragments smaller than first apparent.
- Additional mesoscale cracking morphologies beyond the traditionally reported ring, radial, conical, and laminar cracking types have been observed as spiral cracking, and with multiple superimposed 3D hourglass-shaped cracking. Such 3D cracking morphologies are generally asymmetric and are not unrelated to traditional cracking forms normally viewed in 2D. Some limited success has been achieved to date with the segmentation of ensemble cracking morphologies. Fragmentation of the ceramic targets is observed but in-situ metrology of the ceramic fragments has yet to be obtained.
- Embedded residual projectile fragments have been segmented and observed in isolation from the opacity of the surrounding host ceramic. Such embedded fragments are observed to have an inner structure

considerably more complex than simply a monotonic tungsten alloy only segment. In addition to multiple smaller constituent projectile fragments, a surrounding volume of intermixed fine debris consisting of both ceramic and projectile rubble is frequently observed. Porosity is often found within the intermixed fragment masses. Such features can be segmented and in-situ size metrology provides dimensions, surface area, and volume of designated fragment masses.

- d. Impact-induced porosity is observed in many instances adjacent to fragment masses along the center line of the projectile path. There is a considerable size scale distribution to this porosity and it is generally inhomogeneous throughout the bulk of the target ceramic. Similar porosity is observed along cracking boundaries as well. The size and location of individual pores are obtainable with XCT diagnostics as well as the spatial and statistical distribution of pore sizes.
- e. Initial developments in the quantification and 3D mapping of the local damage fraction has been successful for the case of axisymmetric damage [4]. However, the observed damage features are generally asymmetrical, and further development work is needed for the 3D asymmetrical mapping of impact damage features. Also, the process of creating the 3D mapping of the impact damage needs to be simplified and its construction accelerated.

4 Summary

XCT diagnostics were demonstrated to provide unprecedented results of the in-situ characterization and visualization of complex ballistic impact damage features. Future developments and refinements of this technology are realistically anticipated. The need exists for this damage diagnostics technology to be integrated into future damage-based computational modeling efforts. The most feasible way for this to occur is to establish collaborative interchanges between the practitioners of both disciplines. Such collaborations can maximize the functionality of both the content and the format of impact damage diagnostic knowledge and accelerate its incorporation into more realistic predictive models.

Acknowledgements

Acknowledgements are gratefully extended to W.H. Green of ARL for the XCT scans, Dr. D. A. Shockey of SRI for making the Al_2O_3 and B_4C targets available, and Dr. C. Reinhart of Volume Graphics GmbH for assistance with the StudioMax v.1.2.1 voxel analysis and visualization software.

References

- [1] J.M. Wells, On the Role of Impact Damage in Armor Ceramic Performance. Proc. of 30th Int. Conf. on Advanced Ceramics & Composites-Advances in Ceramic Armor, (2006), (In Press)



- [2] J.M. Wells, Progress in the Nondestructive Analysis of Impact Damage in TiB₂ Armor Ceramics. Proc. of 30th International Conf. on Advanced Ceramics & Composites-Advances in Ceramic Armor, 2006, (In Press)
- [3] J. M. Wells, Progress on the NDE Characterization of Impact Damage in Armor Materials. Proc. of 22nd Int. Ballistics Symp., ADPA, v2, pp. 793-800, 2005.
- [4] H.T. Miller, W.H. Green, N. L. Rupert, and J.M. Wells, Quantitative Evaluation of Damage and Residual Penetrator Material in Impacted TiB₂ Targets Using X-Ray Computed Tomography. 21st Int. Symp. on Ballistics, Adelaide, Au, ADPA, v1, pp. 153-159, 2004.
- [5] J. M. Wells, N. L. Rupert, and W. H. Green, Progress in the 3-D Visualization of Interior Ballistic Damage in Armor Ceramics. Ceramic Armor Materials by Design, Ed. J.W. McCauley et al., Ceramic Transactions, v134, ACERS, pp. 441-448, 2002.
- [6] J.M. Wells, On Incorporating XCT into Predictive Ballistic Impact Damage Modeling. Proc. of 22nd Int. Ballistics Symp., ADPA, v2, pp. 1223-1230, 2005.
- [7] J.M. Wells, On Continuing the Evolution of XCT Engineering Capabilities for Impact Damage Diagnostics, Proc. 31st Intern'l Conf. on Advanced Ceramics & Composites, ACERS, 2007, In Press.
- [8] J.M. Wells, N.L. Rupert, W.J. Bruchey, and D.A. Shockey, XCT Diagnostic Evaluation of Ballistic Impact Damage in Confined Ceramic Targets. 23rd Intern'l Symp. on Ballistics, Tarragona, Spain, ADPA v2, 2007, In Press
- [9] J.M. Wells, W.H. Green, N.L. Rupert, J. R. Wheeler, S.J. Cimpoeu, and A.V. Zibarov, Ballistic Damage Visualization & Quantification in Monolithic Ti-6Al-4V with X-ray Computed Tomography. 21st Int. Symp. on Ballistics, DSTO, Adelaide, Australia, ADPA 1, pp. 125-131, 2004.
- [10] T.J. Holmquist and G.R. Johnson, Modeling Prestressed Ceramic and its Effect on Ballistic Performance. Int. Jnl. of Impact Eng'g, 31, pp. 113-127, 2005.
- [11] Volume Graphics StudioMax v1.2.1, www.volumegraphics.com
- [12] D.A. Shockey, A.H. Marchand, S.R. Skaggs, G.E. Cort, M.W. Burkett and R. Parker, Failure Phenomenology of Confined Ceramic Targets and Impacting Rods. Int. Jnl of Impact Eng'g, 9 (3), pp. 263-275, 1990.
- [13] D.A. Shockey, D.R. Curran, R.W. Klopp, L. Seaman, C.H. Kanazawa, and J.T. McGinn. Characterizing and Modeling Penetration of Ceramic Armor. ARO Report No. 30488-3-MS, 1995.
- [14] D.A. Shockey, A.H. Marchand, S.R. Skaggs, G.E. Cort, M.W. Burkett and R. Parker, Failure Phenomenology of Confined Ceramic Targets and Impacting Rods, Ceramic Armor Materials by Design, Ed. J.W. McCauley et al., Ceramic Transactions, v134, ACERS, pp. 385-402 2002.

